

Probing the Higgs boson through Yukawa force

Avik Banerjee¹, Gautam Bhattacharyya²

Saha Institute of Nuclear Physics, HBNI, 1/AF Bidhan Nagar, Kolkata 700064, India

Abstract

The ATLAS and CMS collaborations of the LHC have observed that the Higgs boson decays into the bottom quark-antiquark pair, and have also established that the Higgs coupling with the top quark-antiquark pair is instrumental in one of the modes for Higgs production. This underlines the discovery of the Yukawa force at the LHC. We demonstrate the impact of this discovery on the Higgs properties that are related to the dynamics of electroweak symmetry breaking. We show that these measurements have considerably squeezed the allowed window for new physics contributing to the Higgs couplings with the weak gauge bosons and the third generation quarks. The expected constraints at the HL-LHC and future Higgs factories are also shown. We project these constraints on the parameter space of a few motivated scenarios beyond the Standard Model. We pick them under two broad categories, namely, the composite Higgs and its RS dual, as well as various types of multi-Higgs models. The latter category includes models with singlet scalars, Type I, II and BGL-type two-Higgs doublet models, and models with scalar triplets *à la* Georgi and Machacek.

1 Introduction

Since the discovery of the Higgs boson in 2012 at the CERN Large Hadron Collider (LHC) [1,2], one of the most notable achievements by the ATLAS and CMS Collaborations has been the measurements of the Yukawa force between the Higgs boson (h) and the third generation quarks (t and b). Although Yukawa interaction was postulated long back in the context of the pion-nucleon scattering, advent of Quantum Chromodynamics showed that it is but an artefact of the strong gauge force. Do the present measurements of $hb\bar{b}$ [3,4] and $ht\bar{t}$ [5,6] couplings constitute a discovery of a fundamental Yukawa force, or, it is again a low energy manifestation of some unknown UV dynamics? Even if the Higgs boson is an elementary object, is it the only neutral scalar that Nature offered us? Precision measurements of these Yukawa couplings can shed important light on both these questions. In the Standard Model (SM), the Yukawa couplings are precisely known in terms of the fermion masses. Any departure would indicate physics beyond the SM (BSM) triggering electroweak symmetry breaking [7–10]. In this paper, we review the status of some BSM physics in the light of the LHC data armed with the new measurements of the Yukawa forces. Since the flavor changing couplings of the 125 GeV Higgs boson are already too constrained, increasingly precise measurements of the flavor diagonal couplings at the LHC are essential to probe the Yukawa structure. In order to quantify the BSM window we employ a χ^2 -analysis using the Higgs signal strength data from the ATLAS and CMS Collaborations. The Run 2 data [11,12] with improved measurements of the $hb\bar{b}$ and $ht\bar{t}$ couplings, compared to what Run 1 could achieve [13–19], penetrate rather deep into the BSM parameter space, leading to new constraints. To show the future prospects, we give projections for these measurements at the high luminosity runs of the LHC (HL-LHC) [20]. We also comment on the expected sensitivities of the Higgs coupling measurements in the proposed International Linear Collider (ILC) [21,22], and circular e^+e^- colliders – CEPC [23–25] and FCC-ee [26]. For our purpose, we employ a simple model independent

¹avik.banerjeesinp@saha.ac.in

²gautam.bhattacharyya@saha.ac.in

phenomenological Lagrangian up to two-derivative order, which essentially captures modification of the Higgs couplings [20, 27, 28]. We also translate the limits of our model independent parameter space to the space of two broad BSM categories, namely, the composite Higgs and multi-Higgs models, under the guise of their different *avatars*, which can address the questions raised above.

2 Theoretical framework

Broadly speaking, two types of BSM physics can modify the Higgs boson couplings:

- Mixing with other spin-0 bosons can alter the Higgs couplings. Examples of this type are found in models with additional $SU(2)_L \times U(1)_Y$ multiplets.
- Higher dimensional operators, obtained by integrating out heavy degrees of freedom, can modify the Higgs couplings. Composite Higgs scenario is a typical example of this type. We note that the absence of any signature of new physics at the LHC, till date, strongly motivates the use of model independent effective field theoretic frameworks, involving only the SM particles as the low energy degrees of freedom. Among the various effective theory frameworks, Standard Model effective field theory [29–35] and strongly interacting light Higgs scenario [36–39] are worth mentioning.

In the present analysis, we use a simple model independent phenomenological Lagrangian, in the broken phase of electroweak symmetry, which captures the modifications of the Higgs couplings arising from both the above sources [20, 27, 28]. We expand the terms in the Lagrangian in powers of h as well as in the number of derivatives. Since our primary interest lies in the production and decay of a single Higgs boson, we will only keep terms up to a single insertion of h . The Lagrangian involving the SM fields after the electroweak symmetry breaking, up to two-derivative terms is given below:

$$\mathcal{L} = \mathcal{L}_{(0)} + \mathcal{L}_{(2)}, \quad (2.1)$$

where the lowest order in derivative $\mathcal{L}_{(0)}$ is given as

$$\mathcal{L}_{(0)} = \frac{h}{v} \left[c_V \left(2M_W^2 W_\mu^\dagger W^\mu + M_Z^2 Z_\mu Z^\mu \right) - \sum_f c_f m_f \bar{f} f \right]. \quad (2.2)$$

The two-derivative terms, which may arise by integrating out the BSM states, are given by

$$\mathcal{L}_{(2)} = -\frac{h}{4\pi v} \left[\alpha_e c_{\gamma\gamma} F_{\mu\nu} F^{\mu\nu} + \alpha_e c_{Z\gamma} Z_{\mu\nu} F^{\mu\nu} - \frac{\alpha_s}{2} c_{gg} G_{\mu\nu}^a G^{a\mu\nu} \right]. \quad (2.3)$$

The coefficients c_i are free parameters capturing the impact of BSM physics, and to be constrained by the experimental data. In the SM, $c_V = c_f = 1$ and $c_{\gamma\gamma} = c_{Z\gamma} = c_{gg} = 0$. We also assume those coefficients to be real, i.e. we assume the 125 GeV Higgs boson to be CP even. Implications of CP odd Higgs couplings have been discussed in [40–42]. The Higgs production cross sections and decay widths, normalized to their SM values, can be expressed solely in terms of these coefficients. Throughout this paper, we fix $c_{Z\gamma} = 0$, since the $h \rightarrow Z\gamma$ data is too constrained from the electroweak precision observables and, not unexpectedly, is still unobserved at the LHC [43, 44]. We will also assume that $c_\tau = c_b$ and $c_c = c_s = c_t$, to simplify the analysis.

3 Analyzing the LHC data

We employ a χ^2 -function as defined below to constrain the coefficients c_i using the LHC data:

$$\chi^2 = \sum_{ij} (\mathcal{O}_{\text{th}}^i(\vec{c}) - \mathcal{O}_{\text{exp}}^i) [\mathcal{C}^{-1}]_{ij} (\mathcal{O}_{\text{th}}^j(\vec{c}) - \mathcal{O}_{\text{exp}}^j). \quad (3.1)$$

Here $\mathcal{O}_{\text{exp}}^i$ denotes the experimentally measured value of an observable, while $\mathcal{O}_{\text{th}}^i(\vec{c})$ is the model prediction dependent on the parameters c_i . The covariance matrix \mathcal{C} captures the experimental uncertainties and correlations among the different observables. For our purpose, we use the individual Higgs signal strength observables (μ), which for a specific process $i \rightarrow h \rightarrow f$ is conventionally defined as

$$\mu_i^f = \frac{\sigma_i B_f}{\sigma_i^{\text{SM}} B_f^{\text{SM}}} = \frac{\sigma_i \Gamma_f \Gamma_h^{\text{SM}}}{\sigma_i^{\text{SM}} \Gamma_f^{\text{SM}} \Gamma_h}, \quad (3.2)$$

where σ_i , Γ_f and B_f denote the cross section of the i^{th} production mode of the Higgs boson, the partial decay width of the Higgs into a final state f , and the corresponding branching ratio, respectively. In the total decay width of the Higgs, Γ_h , we shall generally assume that the Higgs can decay only to the SM particles. Towards the end, however, we shall comment on the possibility of the Higgs boson having a non-vanishing branching fraction to invisible decay modes. In terms of the ‘ κ -framework’ [45, 46], we can express the cross-sections and decay widths normalized to their SM values as

$$\frac{\sigma_i}{\sigma_i^{\text{SM}}} = \kappa_i^2, \quad \frac{\Gamma_f}{\Gamma_f^{\text{SM}}} = \kappa_f^2. \quad (3.3)$$

The mapping between the κ -framework and the coefficients c_i can be found in [47]. We minimize the χ^2 -function to find the best-fit points and draw contours corresponding to $\Delta\chi^2 = \chi^2 - \chi_{\text{min}}^2 = 2.3$ (5.99) denoting regions allowed by 68% (95%) CL in the two dimensional parameter space. We also define new observables by normalizing all the signal strengths by that of the gold-plated $gg \rightarrow h \rightarrow ZZ^*$ process, measured with maximum precision. This way the inherent uncertainties in the total decay width of the Higgs coming from possible invisible modes get eliminated. The other advantage is that, if we assume only the SM particles are running inside the loops for processes like $gg \rightarrow h$ and $h \rightarrow \gamma\gamma$, all the ratios can be expressed in terms of only two variables, *viz.* c_t/c_V and c_b/c_V . Then the constraints from the Higgs signal strength measurements can be represented in a two-dimensional $c_b/c_V - c_t/c_V$ plane. Admittedly, even if the Γ_h dependence is eliminated in this approach, the errors and correlations among the ratios of signal strengths get slightly jacked up compared to the approach where we have analyzed individual signal strengths.

In this paper we primarily work with the LHC Higgs data available till date. In particular, we use ATLAS Run 2 data with 80 fb^{-1} luminosity [11] and CMS Run 2 data with 137 fb^{-1} luminosity [12]. For the purpose of comparison, we also show the results obtained from the combined ATLAS and CMS Run 1 data [13]. As for the HL-LHC projections, with luminosity 3000 fb^{-1} , we use the SM predictions as central values, and the uncertainties expected to be achieved at the end of the HL-LHC program as reported in [20]. Finally we make some estimates of the expected precision of the Higgs coupling measurements using the reported sensitivities at the ILC ($\sqrt{s} = 250 \text{ GeV}$, $\mathcal{L} = 1.2 \text{ ab}^{-1}$ [22]), CEPC ($\sqrt{s} = 250 \text{ GeV}$, $\mathcal{L} = 5.6 \text{ ab}^{-1}$, [25]) and FCC-ee ($\sqrt{s} = 240 \text{ GeV}$, $\mathcal{L} = 5 \text{ ab}^{-1}$, [26]). For the clarity of presentation, we compiled the data used in this analysis in Table 2 of Appendix A. Some crucial observations regarding the present data are the following. First, the processes involving $t\bar{t}h$ production mode have been measured with unprecedented precision at Run 2. Similarly, the errors for the $h\bar{b}b$ decay channels have got significantly reduced, in particular in the associated Higgs production channel. Besides, $gg \rightarrow h \rightarrow \gamma\gamma$ and $gg \rightarrow h \rightarrow ZZ^*$ processes, which were already measured with less

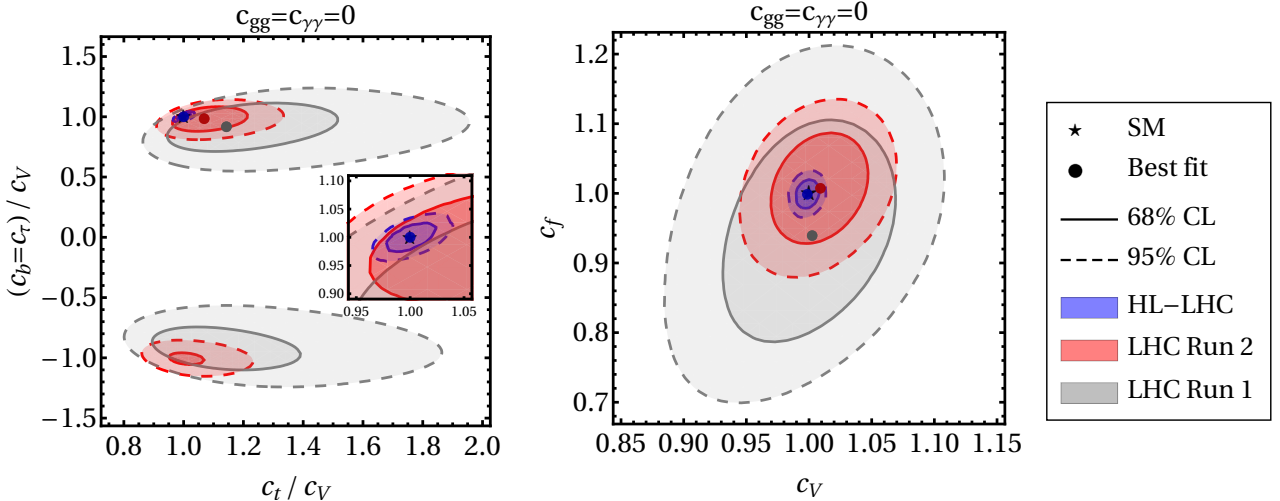


Figure 1: In the left panel, the allowed regions in the plane of c_b/c_V and c_t/c_V are shown at 68% CL (area inside the solid lines) and 95% CL (area inside the dashed lines). We use the ratios of signal strengths from the Run 1 (grey) and Run 2 (red) LHC data, as well as the HL-LHC projections (blue), to extract the limits. The HL-LHC projection is magnified and shown in the inset. In the right panel, we use the individual signal strengths and put limits on $c_t = c_b = c_\tau = c_f$ and c_V . While plotting, $c_{gg} = c_{\gamma\gamma} = 0$ is assumed.

than 30% errors in the Run 1 phase, now stand better with around 15% errors after the Run 2 data were analyzed. While combining ATLAS and CMS Run 2 data, we assume them to be independent of each other and give equal weightage to both the datasets in the χ^2 -function. However, the correlations between the various signal strengths, given by individual collaborations are included in the fit through the matrix \mathcal{C} .

4 Results

It has been shown in [27, 48, 49] that the LEP data admit around 10% – 20% deviation in c_V from its SM value at 95% CL. In the present analysis we have observed that the current Higgs signal strength data provide competitive, if not better, limits on c_V .

The parameter c_t receives major constraints from the gluon fusion and $t\bar{t}h$ production modes of the Higgs boson as well as from its diphoton decay channel. On the other hand, constraints on c_b primarily arise from the $h \rightarrow b\bar{b}$ decay (58% branching ratio). Moreover, since we have assumed $c_b = c_\tau$ in our analysis, data from the $h \rightarrow \tau^+\tau^-$ channel also contribute to the limits on c_b . We show in the left panel of Fig. 1 the allowed region in the $c_b/c_V - c_t/c_V$ plane, obtained using the ratios of the signal strengths ($\mu_i^f/\mu_{gg}^{ZZ^*}$). The clear improvement from Run 1 to Run 2 is a direct consequence of more precise measurements of $ht\bar{t}$ and $hb\bar{b}$ couplings.

In the right panel of Fig. 1, we use the conventional approach of using the individual signal strengths to extract the limits. Here we assume $c_t = c_b = c_\tau = c_f$ to show the allowed region in the $c_f - c_V$ plane. Our results for Run 1 are consistent with those found in [47], validating our fitting method. For the Run 2 data we find $\chi_{\min}^2 = 21.53$ and $\chi_{\text{SM}}^2 - \chi_{\min}^2 < 1$, indicating that the SM fits the data very well. In Table 1 we display the allowed ranges of parameters at 95% CL. Two major points are worth noting here. First, the limits on c_V from the Run 2 data are already competitive to those obtained from the electroweak precision tests. This happened primarily due to the increasingly precise

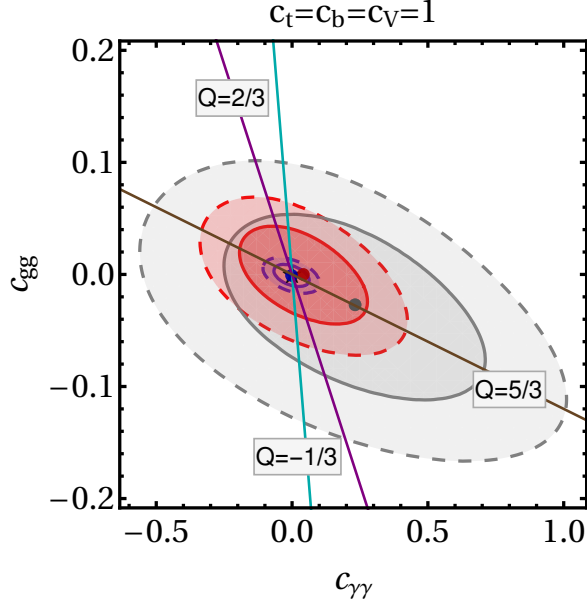


Figure 2: Constraints on $c_{gg} - c_{\gamma\gamma}$ plane at 95% CL are displayed. The solid cyan, purple and brown lines denote the contributions to ggh and $h\gamma\gamma$ triangle loops by color triplet BSM particles with electric charges $Q = -1/3$, $Q = 2/3$ and $Q = 5/3$, respectively. We have fixed $c_f = c_V = 1$. The color codes are: Run 1 (grey), Run 2 (red), HL-LHC (blue).

Figure	Quantity	Run 1	Run 2	HL-LHC
Fig. 1 left panel	c_b/c_V	[0.55 – 1.24]	[0.81 – 1.14]	[0.95 – 1.05]
	c_t/c_V	[0.86 – 1.96]	[0.91 – 1.33]	[0.96 – 1.05]
Fig. 1 right panel	c_f	[0.70 – 1.21]	[0.88 – 1.14]	[0.96 – 1.04]
	c_V	[0.88 – 1.11]	[0.95 – 1.07]	[0.98 – 1.02]
Fig. 2	c_{gg}	[-0.17 – 0.10]	[-0.07 – 0.07]	[-0.02 – 0.02]
	$c_{\gamma\gamma}$	[-0.57 – 1.02]	[-0.34 – 0.43]	[-0.11 – 0.11]

Table 1: The range of allowed values for different coupling modification parameters at 95% CL, extracted from the Figs. 1 and 2, are tabulated. Though there are two disjoint sets of limits on c_b , one on positive and the other on negative side, as evident from the left panel of Fig. 1, for brevity we display in this Table the positive side range only. Assuming $c_b = c_t = c_f$, the allowed 95% CL ranges of c_f/c_V are obtained using the ratios of signal strengths as: Run 1: [0.86 – 1.22], Run 2: [0.92 – 1.13], HL-LHC: [0.97 – 1.03].

measurements of the $gg \rightarrow h \rightarrow ZZ^*$ and $gg \rightarrow h \rightarrow WW^*$ processes. Second, the window for new physics through c_f has significantly narrowed down, only 10% – 15% deviation is allowed from the SM reference point. This improvement in Yukawa force measurement helps discriminate various BSM scenarios. We note that the combined Run 1 + Run 2 data improve the limits obtained from Run 2 data alone by at most 2% – 3%. While future e^+e^- colliders can directly measure the hVV and $hb\bar{b}$ couplings with much higher precision, $ht\bar{t}$ coupling will get constrained only indirectly. We have estimated that at the future Higgs factories like ILC (CEPC), the uncertainties on c_V and c_f would be around 0.01 (0.004) and 0.03 (0.009) at 95% CL, respectively. In FCC-ee as well, the uncertainties would reduce by almost an order of magnitude to $\mathcal{O}(10^{-3})$ in comparison to HL-LHC. In obtaining

the above constraints we have assumed $c_{gg} = c_{\gamma\gamma} = 0$. The inherent assumption is that any new BSM particle(s) which might have contributed to the triangle loops creating the effective ggh and $h\gamma\gamma$ vertices are sufficiently heavy and decoupled.

Then we go to the other extreme. Keeping $c_b = c_t = c_\tau = c_V = 1$, we display the limits in $c_{gg} - c_{\gamma\gamma}$ plane in Fig. 2. Here we capture the effects of the new BSM particles floating in the triangle loops, e.g. if the SM is extended with additional colored and electrically charged particles. The solid lines represent the contributions from colored particles, transforming as triplets of $SU(3)_c$ and having electric charges $Q = -1/3$ (cyan), $Q = 2/3$ (purple) and $Q = 5/3$ (brown), respectively. The exact location of a model-point on each straight line, however, depends on the mass and model-dependent couplings of the new particles with the Higgs boson [27].

If a non-vanishing branching fraction for the invisible decay mode (B_{inv}) of the Higgs boson is admitted, all the individual signal strengths of the Higgs boson receive a scaling by an overall factor of $(1 - B_{\text{inv}})$. Assuming $c_f = c_V = 1$ and $c_{gg} = c_{\gamma\gamma} = 0$, we observe that the Run 1 (Run 2) data exclude $B_{\text{inv}} \gtrsim 18\%$ (8%), while the HL-LHC (ILC/CEPC/FCC-ee) would exclude $B_{\text{inv}} \gtrsim 3\%$ (1%). Admittedly, these limits will relax considerably, if deviations in c_i parameters are allowed (e.g. the Particle Data Group excludes a rather conservative $B_{\text{inv}} \gtrsim 24\%$ [50]).

4.1 Composite Higgs models

In generic composite Higgs scenario, the modification in the hVV coupling is universal [51, 52]

$$c_V = \sqrt{1 - \xi}, \quad (4.1)$$

where $\xi = v^2/f^2$ parametrizes the hierarchy between the electroweak scale and the composite scale f . The Yukawa couplings, however, depend on the details of the particular model. In the minimal composite Higgs model, with coset $SO(5)/SO(4)$ [53–55], the Yukawa coupling modifiers are controlled by the specific representations of $SO(5)$ in which the SM quarks and leptons are embedded. A generic parametrization for c_f in such cases can be given as

$$c_f = 1 + \Delta_f \xi, \quad (4.2)$$

where Δ_f is a free parameter which depends on the number of Yukawa operators. If only one Yukawa operator exists, as in cases where the SM fermions are embedded in **4**, **5** or **10** of $SO(5)$, c_f is determined only by ξ [56–61]. For example, if the top quark is embedded in the fundamental **5** of $SO(5)$ (MCHM₅), we find $\Delta_t = -3/2$, while putting the top in spinorial **4** (MCHM₄), we obtain $\Delta_t = -1/2$. When more than one operator can be constructed, Δ_f depends on the microscopic parameters of the composite dynamics. Such possibilities may occur when either of the left- or right-handed fermions are embedded in the symmetric **14** dimensional representations of $SO(5)$ [60, 62–67].

Here we discuss three specific cases for which we have obtained new limits:

- $\Delta_t = \Delta_b = \Delta_\tau = -3/2$ (MCHM₅): This is an oft-quoted example when both the left- and right-chiral top quark are kept in **5** of $SO(5)$, necessarily yielding $c_{f,V} < 1$. In this case, the χ^2 -function depends on a single parameter ξ . The constraints from Run 2 data are slightly stronger than expectation as the data show a small bias towards the $c_{f,V} > 1$ region (see right panel of Fig. 1). We obtain $f \gtrsim 1.03$ TeV at 95% CL using the Run 2 data, while in HL-LHC we expect $f \gtrsim 1.8$ TeV. In proposed Higgs factories this limit is expected to be further strengthened as $f \gtrsim 2.4$ TeV (ILC), $f \gtrsim 3.3$ TeV (CEPC), and $f \gtrsim 3.1$ TeV (FCC-ee).

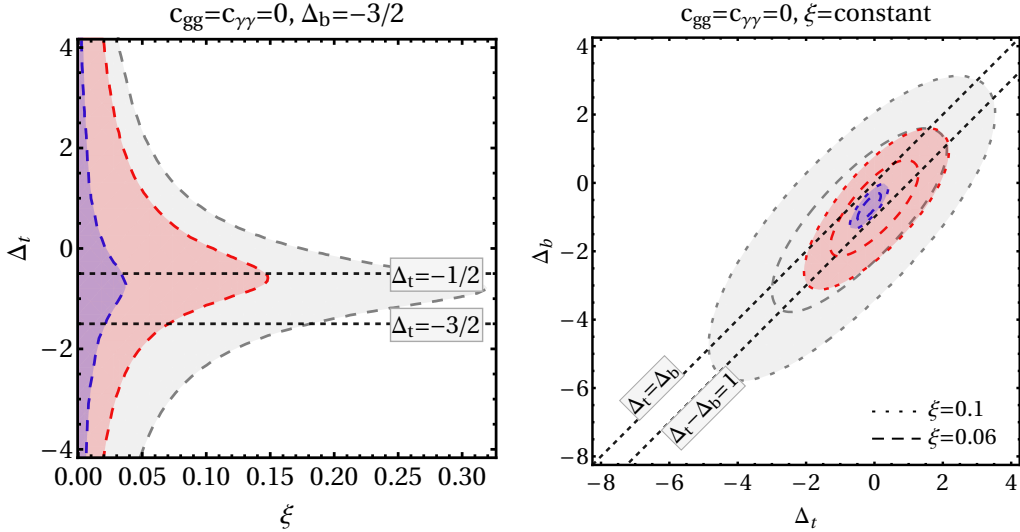


Figure 3: The 95% CL allowed regions for minimal composite Higgs models are shown. In left panel, we fixed $\Delta_b = -3/2$, while in the right panel, we chose $\xi = 0.1$ (dotted) and $\xi = 0.06$ (dashed). The horizontal black dashed lines in the left panel correspond to $\Delta_t = -1/2$ (MCHM₄), and $\Delta_t = -3/2$ (MCHM₅). In the right panel, similar lines represent the contours of $\Delta_t - \Delta_b = 0, 1$. The color codes are: Run 1 (grey), Run 2 (red), HL-LHC (blue).

- $\Delta_b = \Delta_\tau = -3/2$: Here, we keep Δ_t as a free parameter, which implies either the left- or the right-handed top quark is embedded in **14** of SO(5). The allowed region at 95% CL in the $\Delta_t - \xi$ plane is shown in the left panel of Fig. 3. Clearly, the constraint on f gets relaxed, as alluded in [67]. For a generic value of Δ_t , we obtain the most conservative limit $f \gtrsim 650$ GeV after inclusion of the Run 2 data.
- $\xi = \text{constant}$: We fix two representative values of $\xi = 0.1$ and 0.06 , to put simultaneous limits in $\Delta_b - \Delta_t$ plane as shown in the right panel of Fig. 3. We observe that while the present data have not yet gathered enough strength to discriminate between the choices of representations in which the top and bottom quarks are embedded, future measurements with better statistical significance can do the job.

We have kept $c_{gg} = c_{\gamma\gamma} = 0$. This is motivated by the observation that in the composite pseudo-Goldstone Higgs scenario the top partner loop contribution cancels against the contribution of the wave function renormalization of the top quark [62, 68]. The current direct search limit on the vector-like top-partners is around $m_* \sim g_* f \gtrsim 1.5$ TeV [69–71]. Considering the strong coupling $1 \ll g_* < 4\pi$, we clearly observe that the Higgs coupling measurements provide somewhat stronger limits on the compositeness scale. However, the limits from the electroweak precision observables remain comparable, *albeit* with additional model dependence coming from incalculable UV dynamics.

Composite Higgs models are often seen as dual to some variants of the weakly coupled warped extra dimensional models using the AdS / CFT correspondence [72]. We take a custodial Randall-Sundrum (RS) setup with the Higgs boson localized near the IR brane to study the constraints on the scale of the Kaluza-Klein states (M_{KK}) [73–77]. Adapting the expressions for the Higgs coupling modifiers from [77], including the Run 2 data, we obtain a conservative lower limit on the mass of the first excited KK-gluon, $M_g \gtrsim 9$ TeV (which translates into $M_{\text{KK}} \gtrsim 3.7$ TeV). The projected limit from HL-LHC is $M_g \gtrsim 13$ TeV.

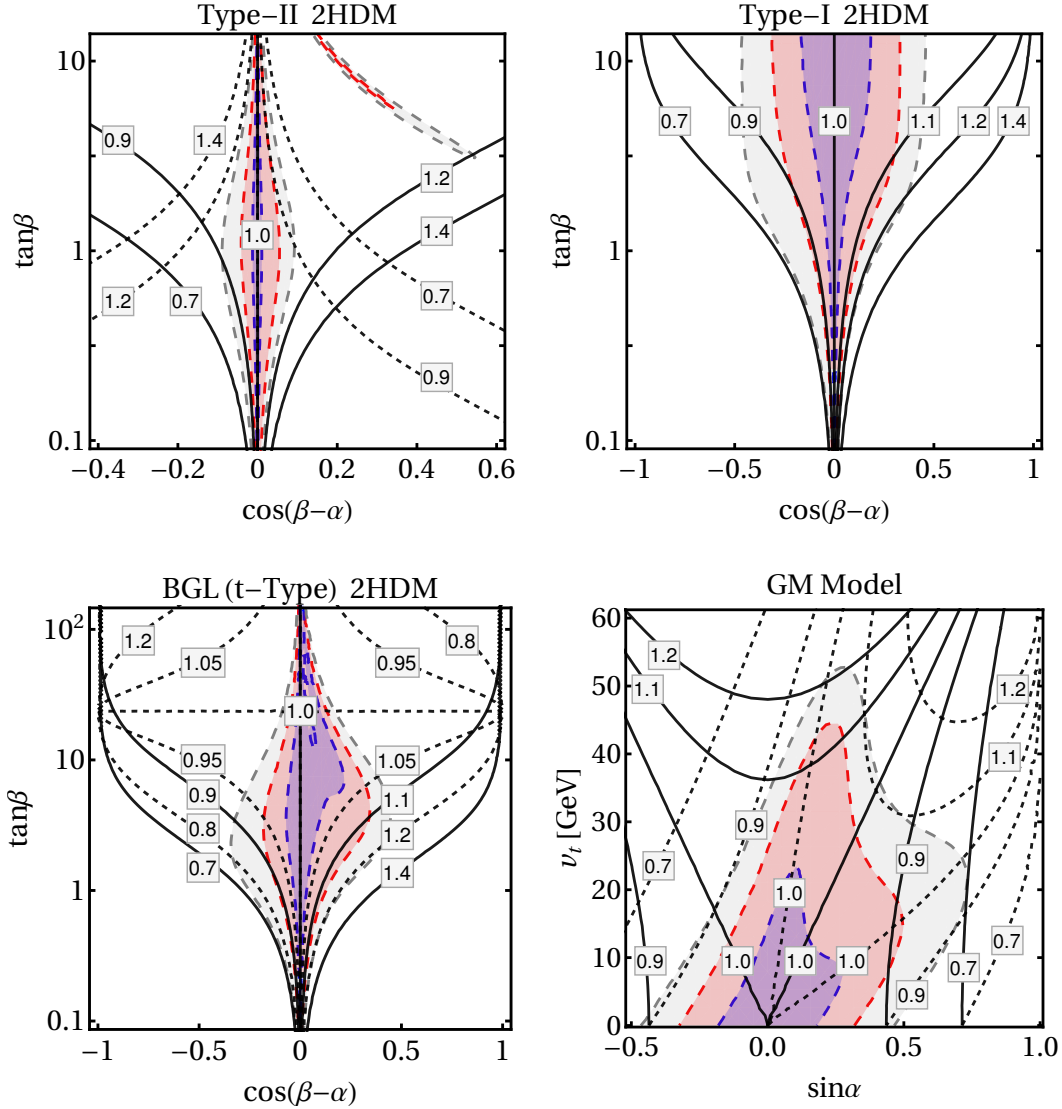


Figure 4: The top-left (top-right) panels show the constraints on parameter space of Type-II (Type-I) 2HDM respectively, while the bottom-left panel corresponds to the BGL (*t*-type) model. For 2HDM, the solid (dashed) black lines denote the contours of constant c_t/c_V (c_b/c_V). The results for Type-I and Type-II 2HDM conform to those obtained in [11, 78]. The bottom-right panel displays the limits on the GM model, for which the solid lines denote the contours for $c_t = c_b$ and the dashed lines denote the same for c_V . The color codes are: Run 1 (grey), Run 2 (red), HL-LHC (blue).

4.2 Multi-Higgs models

Here we deal with theories involving multiple Higgs bosons with non-trivial $SU(2)_L \times U(1)_Y$ charges. The question is whether the 125 GeV Higgs boson discovered at the LHC is the only one of its genre. Since a long time, searches for additional Higgs multiplets are going on in colliders including the LHC. The most trivial extension of the SM is the addition of a gauge singlet CP-even scalar boson [79–82]. Due to the ensuing doublet-singlet scalar mixing, parametrized by an angle α , the 125 GeV Higgs couplings pick up a factor of $\cos \alpha$. At 95% CL, from Run 1 (Run 2) data we obtain $\sin \alpha \lesssim 0.43$ (0.28), while the HL-LHC expectation is $\sin \alpha \lesssim 0.17$. The estimated limits in case of future Higgs factories are $\sin \alpha \lesssim 0.11$ for ILC, while $\sin \alpha \lesssim 0.09$ for CEPC and FCC-ee.

Now we focus on two-Higgs doublet models (2HDM) [83–92]. The hVV coupling modifications in 2HDM depend on two mixing angles as

$$c_V = \sin(\beta - \alpha). \quad (4.3)$$

Above, the angle β parametrizes the mixing between the two doublets, while α is a measure of mass-mixing between the two CP even neutral scalars. In Type-II 2HDM, which also forms the basis of constructing the minimal supersymmetric standard model, the Yukawa coupling modifiers are given by

$$c_t = \frac{\cos \alpha}{\sin \beta}, \quad c_b = -\frac{\sin \alpha}{\cos \beta}. \quad (4.4)$$

Note that, $c_t \neq c_b$ in this case. We have shown the limits on $\tan \beta$ and $\cos(\beta - \alpha)$ in the top-left panel of Fig. 4. The narrow window of allowed region around the alignment limit $\beta - \alpha = \pi/2$ has shrunk considerably with respect to earlier data. In Type-I 2HDM, however, the top and bottom Yukawa couplings are modified by the same factor as

$$c_t = c_b = \frac{\cos \alpha}{\sin \beta}. \quad (4.5)$$

In this case, constraints are displayed in the top-right panel of Fig. 4. The results we found for both Type-I and Type-II 2HDM are compatible with those reported in [11, 78]. The direct searches of heavy Higgs (H) and pseudoscalar Higgs (A) bosons furnish a complementary tool to constrain the 2HDM parameter space. Around the alignment limit, which seems to be strongly favored by the Higgs data, the sensitivity of the direct search limits is poor [90]. Away from the alignment zone and for a heavy Higgs mass $m_H \lesssim 1$ TeV, $H \rightarrow hh$ (above the di-Higgs threshold) and $H \rightarrow VV$, $H \rightarrow \tau^+ \tau^-$ channels provide dominant constraints. The limits for the pseudoscalar Higgs search are important for $m_A \lesssim 1$ TeV, similar to that of heavy Higgs. A special category of 2HDM postulated by Branco, Grimus and Lavoura (the BGL scenario) admits flavor changing neutral current interactions at the tree level, suppressed by the elements of the Cabibbo-Kobayashi-Maskawa (CKM) matrix [93–95]. In some variants of the BGL model (t-type), the expression for c_t resembles that of Type-I 2HDM, while c_b receives an additional contribution proportional to $(\tan \beta + \cot \beta)$ as follows [94]:

$$c_t = \frac{\cos \alpha}{\sin \beta}, \quad c_b = \frac{\cos \alpha}{\sin \beta} - \cos(\beta - \alpha) (\tan \beta + \cot \beta) (1 - |V_{tb}|^2). \quad (4.6)$$

In the low $\tan \beta \lesssim 1$ regime, the constraints on the BGL (t-type) model follow that of the Type-I scenario (see the bottom-left panel of Fig. 4). But with the increasing $\tan \beta \gg 10$, owing to the second term in c_b in Eq. (4.6), tighter limits are obtained compared to the Type-I model. Notably, the LHC data provide complementary constraints in the low $\tan \beta$ region, which is otherwise less sensitive to the flavor observables [94].

Next, we discuss the triplet-extended scenarios, in particular Georgi-Machacek (GM) model [87, 96–104]. In this model the custodial symmetry is protected by the tree level scalar potential, even if the triplets receive a vev (v_t). Without going into the details of the model, we give the expressions for c_V , c_t and c_b for this case as

$$c_V = \cos \alpha \cos \beta + 2\sqrt{\frac{2}{3}} \sin \alpha \sin \beta, \quad c_t = c_b = \frac{\cos \alpha}{\cos \beta}. \quad (4.7)$$

The limits obtained using the Run 1 and Run 2 data from the LHC and the HL-LHC projections are shown in the $v_t - \sin \alpha$ plane in the bottom-right panel of Fig. 4. In analogy to the 2HDM scenario, here also the Higgs data give stronger constraints around $\sin \alpha \sim 0$ in comparison to the limits coming from the direct searches of the heavy states [103].

A few comments on our analysis are in order. First, in deriving these constraints for 2HDM and the GM model, we assumed that the contribution of the charged Higgs bosons decouple in the $h\gamma\gamma$ decay width and thus can be neglected. However, as shown in [105, 106] the decoupling of the charged Higgs contribution to diphoton decay channel depends on the details of the particular model in question. Indeed, our limits would change accordingly. Second, the limits are obtained assuming only renormalizable interactions. The presence of higher dimensional operators [39, 67, 107–112] would lead to further modifications of all the couplings in addition to what comes out of the mixing in the renormalizable setup. As shown in [113] in the context of 2HDM and in [112] for the GM model, these additional modifications, seeping through extra coefficients, would leave indelible imprint on the ranges of the model parameters.

5 Conclusions and outlook

We summarize below the important points raised in this paper. The LHC Run 2 data contain a significantly improved information on the Yukawa couplings. Their inclusion has allowed us to extract important limits.

- The ATLAS and CMS Collaborations have made an important breakthrough in getting a grip on the Yukawa force for the first time. If the Higgs boson turns out to be elementary, then it signifies the observation of a new fundamental force. The experimental measurements have made a huge impact in constraining the allowed region of BSM physics manifesting through modified Yukawa couplings. The Run 2 data are particularly instrumental in squeezing the 2σ BSM window in the Yukawa couplings from 25% to 15% around their SM values when compared to the performance of the Run 1 data. HL-LHC would bring it down to within 5%. The limits on hVV ($V = W, Z$) couplings from the LHC are now competitive with those obtained from electroweak precision tests. The Run 1 (Run 2) data allow not more than 18% (8%) of the total branching fraction of the Higgs boson in the invisible channel. However, larger leak into invisible mode can be accommodated if the hVV and $hff\bar{f}$ couplings substantially deviate from their SM reference points.
- We consider a few motivated BSM scenarios and recast the constraints from our model independent analysis on the parameter space of those specific models using the latest Higgs data. We have observed that, in the context of the SO(5)/SO(4) minimal composite Higgs model, more precise measurements of Yukawa forces have improved the limits on the compositeness scale. The limits depend on the representations of SO(5) in which we embed the left- and right-chiral top quark. At 95% CL, our new limits are

$$f \gtrsim 650 \text{ GeV (most conservative)}, \quad f \gtrsim 1.03 \text{ TeV (MCHM}_5\text{)}.$$

We have shown how the future HL-LHC data would further sharpen the limits. In the RS scenarios with the Higgs boson localized near the IR brane, the first excited KK-gluon weighs more than $\mathcal{O}(10)$ TeV. The exact limit depends on the details of the model parameters.

- The amount of mixing between the SM Higgs with any additional scalar singlet is observed to be rather constrained by the present data, given by $\sin\alpha \lesssim 0.28$. For Type-II 2HDM, only a narrow region around the alignment limit is acceptable, while for the Type-I case a considerable area in the large $\tan\beta$ region is still allowed. In the BGL (t-type) model the constraints in the low $\tan\beta \lesssim 1$ region are in the same ballpark as in the Type-I scenario, while for $\tan\beta \gg 10$ the BGL (t-type) receives stronger constraints than Type-I. We have also shown that for the

Georgi-Machacek model $v_t \lesssim 45$ GeV and $-0.3 \lesssim \sin \alpha \lesssim 0.5$ are allowed by the present data. If data continue to push the Higgs couplings towards the SM values, certain scenarios might still accommodate additional light scalars as allowed by the current direct search limits.

- We have considered the inclusive Higgs cross sections to constrain the anomalous Higgs couplings. However, in some cases, differential distribution may provide additional information. Notably, the degeneracy between c_t and c_{gg} may be lifted using differential distribution data [114–116]. Admixture of CP-odd component to the Higgs can in principle be probed using precise analysis of the final state angular distribution [117, 118]. On the other hand, measurement of the off-shell Higgs production can shed some light on the energy dependence of the couplings [119, 120].
- Once the HL-LHC data become available, a better handle on the Yukawa couplings, including those involving other fermions (e.g. τ lepton), would unravel even inner layers of underlying dynamics. Moreover the future Higgs factories are expected to reduce the uncertainties in the Higgs couplings from percentage to per-mille level, thus probing deeper into the BSM parameter space.

Acknowledgments

A.B. acknowledges support from the Department of Atomic Energy, Government of India. G.B. acknowledges support of the J.C. Bose National Fellowship from the Department of Science and Technology, Government of India (SERB Grant No. SB/S2/JCB-062/2016).

A Higgs signal strength data

We collect the Higgs signal strength data that we have used to perform the χ^2 -fitting from the references [11–13, 20], which we tabulate below. The covariance matrices are taken from the published papers for the ATLAS Run 2 data (Fig. 6 of [11]) and ATLAS + CMS combined Run 1 data (Fig. 27 of [13]), while for the CMS Run 2 data it is collected from the supplementary materials available online³. Further note that for the HL-LHC projections the central values are taken as 1.0 for each of the signal strengths and the uncertainties correspond to the projected sensitivities at the end of the HL-LHC program (‘S2’ dataset of [20]). Since the total uncertainties for the CMS projections for HL-LHC have not been reported, we have added the statistical and systematic parts in quadrature. The uncertainty projections for the future Higgs factories are extracted from Table 5.5 of [22] for ILC, Table 11 of [25] for CEPC and Table 4.1 of [26] for FCC-ee.

³<http://cms-results.web.cern.ch/cms-results/public-results/preliminary-results/HIG-19-005/index.html>

Production	Decay	Run 1	Run 2		HL-LHC [20]	
		ATLAS+CMS [13]	ATLAS [11]	CMS [12]	ATLAS	CMS
ggH	$\gamma\gamma$	$1.10^{+0.23}_{-0.22}$	0.96 ± 0.14	$1.09^{+0.15}_{-0.14}$	± 0.04	± 0.04
	ZZ	$1.13^{+0.34}_{-0.31}$	$1.04^{+0.16}_{-0.15}$	$0.98^{+0.12}_{-0.11}$	± 0.04	± 0.04
	WW	0.84 ± 0.17	1.08 ± 0.19	$1.28^{+0.20}_{-0.19}$	$+0.05_{-0.04}$	± 0.03
	$\tau^+\tau^-$	1.00 ± 0.60	$0.96^{+0.59}_{-0.52}$	$0.39^{+0.38}_{-0.39}$	$+0.12_{-0.11}$	± 0.06
	$b\bar{b}$	–	–	$2.45^{+2.53}_{-2.35}$	–	–
VBF	$\gamma\gamma$	1.30 ± 0.50	$1.39^{+0.40}_{-0.35}$	$0.77^{+0.37}_{-0.29}$	$+0.10_{-0.09}$	± 0.14
	ZZ	$0.10^{+1.10}_{-0.60}$	$2.68^{+0.98}_{-0.83}$	$0.57^{+0.46}_{-0.36}$	± 0.12	± 0.18
	WW	1.20 ± 0.40	$0.59^{+0.36}_{-0.35}$	$0.63^{+0.65}_{-0.61}$	$+0.10_{-0.09}$	± 0.09
	$\tau^+\tau^-$	1.30 ± 0.40	$1.16^{+0.58}_{-0.53}$	$1.05^{+0.30}_{-0.29}$	± 0.08	± 0.06
	$b\bar{b}$	–	$3.01^{+1.67}_{-1.61}$	–	–	–
VH	$\gamma\gamma$	–	$1.09^{+0.58}_{-0.54}$	–	± 0.09	–
	ZZ	–	$0.68^{+1.20}_{-0.78}$	–	$+0.19_{-0.18}$	–
	WW	–	–	–	–	–
	$\tau^+\tau^-$	–	–	–	–	–
	$b\bar{b}$	–	$1.19^{+0.27}_{-0.25}$	–	–	± 0.06
WH	$\gamma\gamma$	$0.50^{+1.30}_{-1.20}$	–	–	–	± 0.20
	ZZ	–	–	$1.10^{+0.96}_{-0.74}$	–	± 0.67
	WW	$1.60^{+1.20}_{-1.00}$	–	$2.85^{+2.11}_{-1.87}$	–	± 0.19
	$\tau^+\tau^-$	-1.4 ± 1.4	–	$3.01^{+1.65}_{-1.51}$	–	–
	$b\bar{b}$	1.00 ± 0.50	–	$1.27^{+0.42}_{-0.40}$	± 0.10	–
ZH	$\gamma\gamma$	$0.50^{+3.00}_{-2.50}$	–	–	–	± 0.33
	ZZ	–	–	$1.10^{+0.96}_{-0.74}$	–	± 1.09
	WW	$5.90^{+2.60}_{-2.20}$	–	$0.90^{+1.77}_{-1.43}$	–	± 0.25
	$\tau^+\tau^-$	$2.20^{+2.20}_{-1.80}$	–	$1.53^{+1.60}_{-1.37}$	–	–
	$b\bar{b}$	0.40 ± 0.40	–	$0.93^{+0.33}_{-0.31}$	± 0.45	–
$t\bar{t}H + tH$	$\gamma\gamma$	–	$1.10^{+0.41}_{-0.35}$	–	–	–
	VV	–	$1.50^{+0.59}_{-0.57}$	–	–	–
	$\tau^+\tau^-$	–	$1.38^{+1.13}_{-0.96}$	–	–	–
	$b\bar{b}$	–	$0.79^{+0.60}_{-0.59}$	–	–	–
$t\bar{t}H$	$\gamma\gamma$	$2.20^{+1.60}_{-1.30}$	–	$1.62^{+0.52}_{-0.43}$	$+0.08_{-0.07}$	± 0.11
	ZZ	–	–	$0.25^{+1.03}_{-0.25}$	$+0.23_{-0.20}$	± 0.33
	WW	$5.00^{+1.80}_{-1.70}$	–	$0.93^{+0.48}_{-0.45}$	–	–
	$\tau^+\tau^-$	$-1.9^{+3.7}_{-3.3}$	–	$0.81^{+0.74}_{-0.67}$	–	–
	$b\bar{b}$	1.10 ± 1.00	–	$1.13^{+0.33}_{-0.30}$	–	–

Table 2: The Higgs signal strength data used to perform the χ^2 -analysis. For the HL-LHC case, only the projected uncertainties are reported assuming the central values to be equal to 1.0.

References

- [1] ATLAS collaboration, G. Aad et al., *Observation of a new particle in the search for the Standard Model Higgs boson with the ATLAS detector at the LHC*, *Phys. Lett.* **B716** (2012) 1–29, [[1207.7214](#)].
- [2] CMS collaboration, S. Chatrchyan et al., *Observation of a new boson at a mass of 125 GeV with the CMS experiment at the LHC*, *Phys. Lett.* **B716** (2012) 30–61, [[1207.7235](#)].
- [3] CMS collaboration, A. M. Sirunyan et al., *Observation of Higgs boson decay to bottom quarks*, *Phys. Rev. Lett.* **121** (2018) 121801, [[1808.08242](#)].
- [4] ATLAS collaboration, M. Aaboud et al., *Observation of $H \rightarrow b\bar{b}$ decays and VH production with the ATLAS detector*, *Phys. Lett.* **B786** (2018) 59–86, [[1808.08238](#)].
- [5] CMS collaboration, A. M. Sirunyan et al., *Observation of $t\bar{t}H$ production*, *Phys. Rev. Lett.* **120** (2018) 231801, [[1804.02610](#)].
- [6] ATLAS collaboration, M. Aaboud et al., *Observation of Higgs boson production in association with a top quark pair at the LHC with the ATLAS detector*, *Phys. Lett.* **B784** (2018) 173–191, [[1806.00425](#)].
- [7] S. Bar-Shalom and A. Soni, *Universally enhanced light-quarks Yukawa couplings paradigm*, *Phys. Rev. D* **98** (2018) 055001, [[1804.02400](#)].
- [8] M. Arroyo-Ureña and J. L. Diaz-Cruz, *Hidden Signals of New Physics within the Yukawa Couplings of the Higgs boson*, *Phys. Lett. B* **810** (2020) 135799, [[2005.01153](#)].
- [9] D. A. Dicus and H.-J. He, *Scales of fermion mass generation and electroweak symmetry breaking*, *Phys. Rev. D* **71** (2005) 093009, [[hep-ph/0409131](#)].
- [10] D. A. Dicus and H.-J. He, *Scales of mass generation for quarks, leptons and majorana neutrinos*, *Phys. Rev. Lett.* **94** (2005) 221802, [[hep-ph/0502178](#)].
- [11] ATLAS collaboration, G. Aad et al., *Combined measurements of Higgs boson production and decay using up to 80 fb^{-1} of proton-proton collision data at $\sqrt{s} = 13$ TeV collected with the ATLAS experiment*, *Phys. Rev.* **D101** (2020) 012002, [[1909.02845](#)].
- [12] CMS collaboration, *Combined Higgs boson production and decay measurements with up to 137 fb^{-1} of proton-proton collision data at $\sqrt{s} = 13$ TeV*, Tech. Rep. CMS-PAS-HIG-19-005, CERN, Geneva, 2020.
- [13] ATLAS, CMS collaboration, G. Aad et al., *Measurements of the Higgs boson production and decay rates and constraints on its couplings from a combined ATLAS and CMS analysis of the LHC pp collision data at $\sqrt{s} = 7$ and 8 TeV*, *JHEP* **08** (2016) 045, [[1606.02266](#)].
- [14] A. Azatov, R. Contino and J. Galloway, *Model-Independent Bounds on a Light Higgs*, *JHEP* **04** (2012) 127, [[1202.3415](#)].
- [15] J. Ellis and T. You, *Updated Global Analysis of Higgs Couplings*, *JHEP* **06** (2013) 103, [[1303.3879](#)].
- [16] M. B. Einhorn and J. Wudka, *Higgs-Boson Couplings Beyond the Standard Model*, *Nucl. Phys. B* **877** (2013) 792–806, [[1308.2255](#)].

- [17] A. Pomarol and F. Riva, *Towards the Ultimate SM Fit to Close in on Higgs Physics*, *JHEP* **01** (2014) 151, [[1308.2803](#)].
- [18] J. de Blas, M. Ciuchini, E. Franco, D. Ghosh, S. Mishima, M. Pierini et al., *Global Bayesian Analysis of the Higgs-boson Couplings*, *Nucl. Part. Phys. Proc.* **273-275** (2016) 834–840, [[1410.4204](#)].
- [19] J. Bernon, B. Dumont and S. Kraml, *Status of Higgs couplings after run 1 of the LHC*, *Phys. Rev. D* **90** (2014) 071301, [[1409.1588](#)].
- [20] M. Cepeda et al., *Report from Working Group 2*, *CERN Yellow Rep. Monogr.* **7** (2019) 221–584, [[1902.00134](#)].
- [21] S. Dawson et al., *Working Group Report: Higgs Boson*, in *Community Summer Study 2013: Snowmass on the Mississippi*, 10, 2013. [1310.8361](#).
- [22] D. Asner et al., *ILC Higgs White Paper*, in *Community Summer Study 2013: Snowmass on the Mississippi*, 10, 2013. [1310.0763](#).
- [23] S.-F. Ge, H.-J. He and R.-Q. Xiao, *Testing Higgs coupling precision and new physics scales at lepton colliders*, [1612.02718](#).
- [24] J. Gu, H. Li, Z. Liu, S. Su and W. Su, *Learning from Higgs Physics at Future Higgs Factories*, *JHEP* **12** (2017) 153, [[1709.06103](#)].
- [25] F. An et al., *Precision Higgs physics at the CEPC*, *Chin. Phys. C* **43** (2019) 043002, [[1810.09037](#)].
- [26] FCC collaboration, A. Abada et al., *FCC Physics Opportunities: Future Circular Collider Conceptual Design Report Volume 1*, *Eur. Phys. J. C* **79** (2019) 474.
- [27] A. Falkowski, F. Riva and A. Urbano, *Higgs at last*, *JHEP* **11** (2013) 111, [[1303.1812](#)].
- [28] G. Buchalla, O. Cata, A. Celis and C. Krause, *Fitting Higgs Data with Nonlinear Effective Theory*, *Eur. Phys. J. C* **76** (2016) 233, [[1511.00988](#)].
- [29] W. Buchmuller and D. Wyler, *Effective Lagrangian Analysis of New Interactions and Flavor Conservation*, *Nucl. Phys.* **B268** (1986) 621–653.
- [30] K. Hagiwara, S. Ishihara, R. Szalapski and D. Zeppenfeld, *Low-energy effects of new interactions in the electroweak boson sector*, *Phys. Rev.* **D48** (1993) 2182–2203.
- [31] B. Grzadkowski, M. Iskrzynski, M. Misiak and J. Rosiek, *Dimension-Six Terms in the Standard Model Lagrangian*, *JHEP* **10** (2010) 085, [[1008.4884](#)].
- [32] J. Ellis, V. Sanz and T. You, *Complete Higgs Sector Constraints on Dimension-6 Operators*, *JHEP* **07** (2014) 036, [[1404.3667](#)].
- [33] S. Jana and S. Nandi, *New Physics Scale from Higgs Observables with Effective Dimension-6 Operators*, *Phys. Lett. B* **783** (2018) 51–58, [[1710.00619](#)].
- [34] I. Brivio and M. Trott, *The Standard Model as an Effective Field Theory*, *Phys. Rept.* **793** (2019) 1–98, [[1706.08945](#)].
- [35] J. Ellis, C. W. Murphy, V. Sanz and T. You, *Updated Global SMEFT Fit to Higgs, Diboson and Electroweak Data*, *JHEP* **06** (2018) 146, [[1803.03252](#)].

- [36] G. F. Giudice, C. Grojean, A. Pomarol and R. Rattazzi, *The Strongly-Interacting Light Higgs*, *JHEP* **06** (2007) 045, [[hep-ph/0703164](#)].
- [37] R. Contino, M. Ghezzi, C. Grojean, M. Muhlleitner and M. Spira, *Effective Lagrangian for a light Higgs-like scalar*, *JHEP* **07** (2013) 035, [[1303.3876](#)].
- [38] G. Buchalla, O. Cata and C. Krause, *A Systematic Approach to the SILH Lagrangian*, *Nucl. Phys. B* **894** (2015) 602–620, [[1412.6356](#)].
- [39] M. Chala, G. Durieux, C. Grojean, L. de Lima and O. Matsedonskyi, *Minimally extended SILH*, *JHEP* **06** (2017) 088, [[1703.10624](#)].
- [40] A. Kobakhidze, N. Liu, L. Wu and J. Yue, *Implications of CP-violating Top-Higgs Couplings at LHC and Higgs Factories*, *Phys. Rev. D* **95** (2017) 015016, [[1610.06676](#)].
- [41] E. Fuchs, M. Losada, Y. Nir and Y. Viernik, *Implications of the Upper Bound on $h \rightarrow \mu^+ \mu^-$ on the Baryon Asymmetry of the Universe*, *Phys. Rev. Lett.* **124** (2020) 181801, [[1911.08495](#)].
- [42] E. Fuchs, M. Losada, Y. Nir and Y. Viernik, *CP violation from τ , t and b dimension-6 Yukawa couplings - interplay of baryogenesis, EDM and Higgs physics*, *JHEP* **05** (2020) 056, [[2003.00099](#)].
- [43] ATLAS collaboration, M. Aaboud et al., *Searches for the $Z\gamma$ decay mode of the Higgs boson and for new high-mass resonances in pp collisions at $\sqrt{s} = 13$ TeV with the ATLAS detector*, *JHEP* **10** (2017) 112, [[1708.00212](#)].
- [44] CMS collaboration, A. M. Sirunyan et al., *Search for the decay of a Higgs boson in the $\ell\ell\gamma$ channel in proton-proton collisions at $\sqrt{s} = 13$ TeV*, *JHEP* **11** (2018) 152, [[1806.05996](#)].
- [45] LHC HIGGS CROSS SECTION WORKING GROUP collaboration, J. R. Andersen et al., *Handbook of LHC Higgs Cross Sections: 3. Higgs Properties*, [1307.1347](#).
- [46] LHC HIGGS CROSS SECTION WORKING GROUP collaboration, D. de Florian et al., *Handbook of LHC Higgs Cross Sections: 4. Deciphering the Nature of the Higgs Sector*, [1610.07922](#).
- [47] J. de Blas, O. Eberhardt and C. Krause, *Current and Future Constraints on Higgs Couplings in the Nonlinear Effective Theory*, *JHEP* **07** (2018) 048, [[1803.00939](#)].
- [48] M. Ciuchini, E. Franco, S. Mishima and L. Silvestrini, *Electroweak Precision Observables, New Physics and the Nature of a 126 GeV Higgs Boson*, *JHEP* **08** (2013) 106, [[1306.4644](#)].
- [49] J. de Blas, M. Ciuchini, E. Franco, S. Mishima, M. Pierini, L. Reina et al., *Electroweak precision observables and Higgs-boson signal strengths in the Standard Model and beyond: present and future*, *JHEP* **12** (2016) 135, [[1608.01509](#)].
- [50] PARTICLE DATA GROUP collaboration, M. Tanabashi et al., *Review of Particle Physics*, *Phys. Rev. D* **98** (2018) 030001.
- [51] D. Liu, I. Low and Z. Yin, *Universal Imprints of a Pseudo-Nambu-Goldstone Higgs Boson*, *Phys. Rev. Lett.* **121** (2018) 261802, [[1805.00489](#)].
- [52] D. Liu, I. Low and Z. Yin, *Universal Relations in Composite Higgs Models*, *JHEP* **05** (2019) 170, [[1809.09126](#)].

- [53] R. Contino, *The Higgs as a Composite Nambu-Goldstone Boson*, in *Physics of the large and the small, TASI 09, proceedings of the Theoretical Advanced Study Institute in Elementary Particle Physics, Boulder, Colorado, USA, 1-26 June 2009*, pp. 235–306, 2011. [1005.4269](#). DOI.
- [54] G. Panico and A. Wulzer, *The Composite Nambu-Goldstone Higgs*, *Lect. Notes Phys.* **913** (2016) pp.1–316, [[1506.01961](#)].
- [55] C. Csaki and P. Tanedo, *Beyond the Standard Model*, in *Proceedings, 2013 European School of High-Energy Physics (ESHEP 2013): Paradfurdo, Hungary, June 5-18, 2013*, pp. 169–268, 2015. [1602.04228](#). DOI.
- [56] R. Contino, Y. Nomura and A. Pomarol, *Higgs as a holographic pseudoGoldstone boson*, *Nucl. Phys.* **B671** (2003) 148–174, [[hep-ph/0306259](#)].
- [57] K. Agashe, R. Contino and A. Pomarol, *The Minimal composite Higgs model*, *Nucl. Phys.* **B719** (2005) 165–187, [[hep-ph/0412089](#)].
- [58] G. Panico and A. Wulzer, *The Discrete Composite Higgs Model*, *JHEP* **09** (2011) 135, [[1106.2719](#)].
- [59] D. Marzocca, M. Serone and J. Shu, *General Composite Higgs Models*, *JHEP* **08** (2012) 013, [[1205.0770](#)].
- [60] M. Carena, L. Da Rold and E. Pontón, *Minimal Composite Higgs Models at the LHC*, *JHEP* **06** (2014) 159, [[1402.2987](#)].
- [61] V. Sanz and J. Setford, *Composite Higgs Models after Run 2*, *Adv. High Energy Phys.* **2018** (2018) 7168480, [[1703.10190](#)].
- [62] M. Montull, F. Riva, E. Salvioni and R. Torre, *Higgs Couplings in Composite Models*, *Phys. Rev.* **D88** (2013) 095006, [[1308.0559](#)].
- [63] A. Carmona and F. Goertz, *A naturally light Higgs without light Top Partners*, *JHEP* **05** (2015) 002, [[1410.8555](#)].
- [64] S. Kanemura, K. Kaneta, N. Machida, S. Odori and T. Shindou, *Single and double production of the Higgs boson at hadron and lepton colliders in minimal composite Higgs models*, *Phys. Rev.* **D94** (2016) 015028, [[1603.05588](#)].
- [65] M. B. Gavela, K. Kanshin, P. A. N. Machado and S. Saa, *The linear–non-linear frontier for the Goldstone Higgs*, *Eur. Phys. J.* **C76** (2016) 690, [[1610.08083](#)].
- [66] D. Liu, I. Low and C. E. M. Wagner, *Modification of Higgs Couplings in Minimal Composite Models*, *Phys. Rev.* **D96** (2017) 035013, [[1703.07791](#)].
- [67] A. Banerjee, G. Bhattacharyya, N. Kumar and T. S. Ray, *Constraining Composite Higgs Models using LHC data*, *JHEP* **03** (2018) 062, [[1712.07494](#)].
- [68] A. Azatov and J. Galloway, *Light Custodians and Higgs Physics in Composite Models*, *Phys. Rev.* **D85** (2012) 055013, [[1110.5646](#)].
- [69] ATLAS collaboration, M. Aaboud et al., *Combination of the searches for pair-produced vector-like partners of the third-generation quarks at $\sqrt{s} = 13$ TeV with the ATLAS detector*, *Phys. Rev. Lett.* **121** (2018) 211801, [[1808.02343](#)].

- [70] ATLAS collaboration, M. Aaboud et al., *Search for new phenomena in events with same-charge leptons and b-jets in pp collisions at $\sqrt{s} = 13$ TeV with the ATLAS detector*, *JHEP* **12** (2018) 039, [[1807.11883](#)].
- [71] CMS collaboration, A. M. Sirunyan et al., *Search for pair production of vectorlike quarks in the fully hadronic final state*, *Phys. Rev. D* **100** (2019) 072001, [[1906.11903](#)].
- [72] J. M. Maldacena, *The Large N limit of superconformal field theories and supergravity*, *Int. J. Theor. Phys.* **38** (1999) 1113–1133, [[hep-th/9711200](#)].
- [73] L. Randall and R. Sundrum, *A Large mass hierarchy from a small extra dimension*, *Phys. Rev. Lett.* **83** (1999) 3370–3373, [[hep-ph/9905221](#)].
- [74] K. Agashe, A. Delgado, M. J. May and R. Sundrum, *RS1, custodial isospin and precision tests*, *JHEP* **08** (2003) 050, [[hep-ph/0308036](#)].
- [75] S. Casagrande, F. Goertz, U. Haisch, M. Neubert and T. Pfoh, *The Custodial Randall-Sundrum Model: From Precision Tests to Higgs Physics*, *JHEP* **09** (2010) 014, [[1005.4315](#)].
- [76] R. Malm, M. Neubert, K. Novotny and C. Schmell, *5D Perspective on Higgs Production at the Boundary of a Warped Extra Dimension*, *JHEP* **01** (2014) 173, [[1303.5702](#)].
- [77] R. Malm, M. Neubert and C. Schmell, *Higgs Couplings and Phenomenology in a Warped Extra Dimension*, *JHEP* **02** (2015) 008, [[1408.4456](#)].
- [78] CMS collaboration, A. M. Sirunyan et al., *Combined measurements of Higgs boson couplings in proton–proton collisions at $\sqrt{s} = 13$ TeV*, *Eur. Phys. J. C* **79** (2019) 421, [[1809.10733](#)].
- [79] T. Robens and T. Stefaniak, *Status of the Higgs Singlet Extension of the Standard Model after LHC Run 1*, *Eur. Phys. J. C* **75** (2015) 104, [[1501.02234](#)].
- [80] T. Robens and T. Stefaniak, *LHC Benchmark Scenarios for the Real Higgs Singlet Extension of the Standard Model*, *Eur. Phys. J. C* **76** (2016) 268, [[1601.07880](#)].
- [81] I. M. Lewis and M. Sullivan, *Benchmarks for Double Higgs Production in the Singlet Extended Standard Model at the LHC*, *Phys. Rev. D* **96** (2017) 035037, [[1701.08774](#)].
- [82] S. Adhikari, I. M. Lewis and M. Sullivan, *Beyond the Standard Model Effective Field Theory: The Singlet Extended Standard Model*, [2003.10449](#).
- [83] G. C. Branco, P. M. Ferreira, L. Lavoura, M. N. Rebelo, M. Sher and J. P. Silva, *Theory and phenomenology of two-Higgs-doublet models*, *Phys. Rept.* **516** (2012) 1–102, [[1106.0034](#)].
- [84] G. Bhattacharyya, D. Das, P. B. Pal and M. Rebelo, *Scalar sector properties of two-Higgs-doublet models with a global U(1) symmetry*, *JHEP* **10** (2013) 081, [[1308.4297](#)].
- [85] N. Craig, J. Galloway and S. Thomas, *Searching for Signs of the Second Higgs Doublet*, [1305.2424](#).
- [86] O. Eberhardt, U. Nierste and M. Wiebusch, *Status of the two-Higgs-doublet model of type II*, *JHEP* **07** (2013) 118, [[1305.1649](#)].
- [87] G. Belanger, B. Dumont, U. Ellwanger, J. F. Gunion and S. Kraml, *Global fit to Higgs signal strengths and couplings and implications for extended Higgs sectors*, *Phys. Rev. D* **88** (2013) 075008, [[1306.2941](#)].

- [88] B. Dumont, J. F. Gunion, Y. Jiang and S. Kraml, *Constraints on and future prospects for Two-Higgs-Doublet Models in light of the LHC Higgs signal*, *Phys. Rev.* **D90** (2014) 035021, [[1405.3584](#)].
- [89] G. Bhattacharyya and D. Das, *Scalar sector of two-Higgs-doublet models: A minireview*, *Pramana* **87** (2016) 40, [[1507.06424](#)].
- [90] D. Chowdhury and O. Eberhardt, *Update of Global Two-Higgs-Doublet Model Fits*, *JHEP* **05** (2018) 161, [[1711.02095](#)].
- [91] J. Ren, R.-Q. Xiao, M. Zhou, Y. Fang, H.-J. He and W. Yao, *LHC Search of New Higgs Boson via Resonant Di-Higgs Production with Decays into $4W$* , *JHEP* **06** (2018) 090, [[1706.05980](#)].
- [92] L.-C. Lü, C. Du, Y. Fang, H.-J. He and H. Zhang, *Searching heavier Higgs boson via di-Higgs production at LHC Run-2*, *Phys. Lett. B* **755** (2016) 509–522, [[1507.02644](#)].
- [93] G. Branco, W. Grimus and L. Lavoura, *Relating the scalar flavor changing neutral couplings to the CKM matrix*, *Phys. Lett. B* **380** (1996) 119–126, [[hep-ph/9601383](#)].
- [94] G. Bhattacharyya, D. Das and A. Kundu, *Feasibility of light scalars in a class of two-Higgs-doublet models and their decay signatures*, *Phys. Rev. D* **89** (2014) 095029, [[1402.0364](#)].
- [95] F. Botella, G. Branco, M. Nebot and M. Rebelo, *Flavour Changing Higgs Couplings in a Class of Two Higgs Doublet Models*, *Eur. Phys. J. C* **76** (2016) 161, [[1508.05101](#)].
- [96] H. Georgi and M. Machacek, *DOUBLY CHARGED HIGGS BOSONS*, *Nucl. Phys.* **B262** (1985) 463–477.
- [97] M. S. Chanowitz and M. Golden, *Higgs Boson Triplets With $M(W) = M(Z) \cos \theta_w$* , *Phys. Lett.* **165B** (1985) 105–108.
- [98] J. F. Gunion, R. Vega and J. Wudka, *Higgs triplets in the standard model*, *Phys. Rev.* **D42** (1990) 1673–1691.
- [99] K. Hartling, K. Kumar and H. E. Logan, *The decoupling limit in the Georgi-Machacek model*, *Phys. Rev.* **D90** (2014) 015007, [[1404.2640](#)].
- [100] K. Hartling, K. Kumar and H. E. Logan, *Indirect constraints on the Georgi-Machacek model and implications for Higgs boson couplings*, *Phys. Rev.* **D91** (2015) 015013, [[1410.5538](#)].
- [101] C.-W. Chiang, S. Kanemura and K. Yagyu, *Novel constraint on the parameter space of the Georgi-Machacek model with current LHC data*, *Phys. Rev.* **D90** (2014) 115025, [[1407.5053](#)].
- [102] C. Degrande, K. Hartling and H. E. Logan, *Scalar decays to $\gamma\gamma$, $Z\gamma$, and $W\gamma$ in the Georgi-Machacek model*, *Phys. Rev.* **D96** (2017) 075013, [[1708.08753](#)].
- [103] C.-W. Chiang, G. Cottin and O. Eberhardt, *Global fits in the Georgi-Machacek model*, [[1807.10660](#)].
- [104] N. Ghosh, S. Ghosh and I. Saha, *Charged Higgs boson searches in the Georgi-Machacek model at the LHC*, *Phys. Rev.* **D101** (2020) 015029, [[1908.00396](#)].
- [105] G. Bhattacharyya and D. Das, *Nondecoupling of charged scalars in Higgs decay to two photons and symmetries of the scalar potential*, *Phys. Rev.* **D91** (2015) 015005, [[1408.6133](#)].

- [106] D. Das and I. Saha, *Cornering variants of the Georgi-Machacek model using Higgs precision data*, *Phys. Rev.* **D98** (2018) 095010, [[1811.00979](#)].
- [107] J. L. Diaz-Cruz, J. Hernandez-Sanchez and J. J. Toscano, *An Effective Lagrangian description of charged Higgs decays $H^+ \rightarrow W^+\gamma$, W^+Z and $W^+ h_0$* , *Phys. Lett.* **B512** (2001) 339–348, [[hep-ph/0106001](#)].
- [108] Y. Kikuta, Y. Okada and Y. Yamamoto, *Structure of dimension-six derivative interactions in pseudo Nambu-Goldstone N Higgs doublet models*, *Phys. Rev.* **D85** (2012) 075021, [[1111.2120](#)].
- [109] A. Crivellin, M. Ghezzi and M. Procura, *Effective Field Theory with Two Higgs Doublets*, *JHEP* **09** (2016) 160, [[1608.00975](#)].
- [110] S. Karmakar and S. Rakshit, *Higher dimensional operators in 2HDM*, *JHEP* **10** (2017) 048, [[1707.00716](#)].
- [111] M. Chala, M. Ramos and M. Spannowsky, *Gravitational wave and collider probes of a triplet Higgs sector with a low cutoff*, *Eur. Phys. J. C* **79** (2019) 156, [[1812.01901](#)].
- [112] A. Banerjee, G. Bhattacharyya and N. Kumar, *Impact of Yukawa-like dimension-five operators on the Georgi-Machacek model*, *Phys. Rev.* **D99** (2019) 035028, [[1901.01725](#)].
- [113] S. Karmakar and S. Rakshit, *Alignment Limit in 2HDM: Robustness put to test*, *JHEP* **09** (2018) 142, [[1802.03366](#)].
- [114] A. Azatov and A. Paul, *Probing Higgs couplings with high p_T Higgs production*, *JHEP* **01** (2014) 014, [[1309.5273](#)].
- [115] C. Grojean, E. Salvioni, M. Schlaffer and A. Weiler, *Very boosted Higgs in gluon fusion*, *JHEP* **05** (2014) 022, [[1312.3317](#)].
- [116] A. Banfi, A. Martin and V. Sanz, *Probing top-partners in Higgs+jets*, *JHEP* **08** (2014) 053, [[1308.4771](#)].
- [117] F. Ferreira, B. Fuks, V. Sanz and D. Sengupta, *Probing CP-violating Higgs and gauge-boson couplings in the Standard Model effective field theory*, *Eur. Phys. J. C* **77** (2017) 675, [[1612.01808](#)].
- [118] F. U. Bernlochner, C. Englert, C. Hays, K. Lohwasser, H. Mildner, A. Pilkington et al., *Angles on CP-violation in Higgs boson interactions*, *Phys. Lett. B* **790** (2019) 372–379, [[1808.06577](#)].
- [119] A. Azatov, C. Grojean, A. Paul and E. Salvioni, *Taming the off-shell Higgs boson*, *Zh. Eksp. Teor. Fiz.* **147** (2015) 410–425, [[1406.6338](#)].
- [120] D. Gonçalves, T. Han and S. Mukhopadhyay, *Higgs Couplings at High Scales*, *Phys. Rev. D* **98** (2018) 015023, [[1803.09751](#)].